

S. Krishtal · M. Kiselev · A. Kolker · A. Idrissi

# Study of H-bond characteristics in sub- and supercritical methanol

Received: 5 July 2005 / Accepted: 12 January 2006 / Published online: 8 November 2006  
© Springer-Verlag 2006

**Abstract** Classical molecular dynamics simulations of various methanol phase lines near the saturation curve and the critical point have been performed to study the changes in H-bonded clusters structure at transition of methanol to supercritical state. Analysis of H-bonds statistics with combined distance-energy H-bond criterion showed that the correlations between topological characteristics of H-bonds and the mole fraction of H-bonded molecules have unique functional representation despite the phase path applied. In the present study, an attempt has been also made to evaluate the degree of hydrogen bonding by combining the DFT computations on classical MD configurations with the natural bond orbital analysis of the waves functions obtained.

**Keywords** Supercritical methanol · H-bonded clusters · Molecular dynamics simulation

## 1 Introduction

It is known from theoretical and experimental studies of sub- and supercritical fluids (SCF) that thermodynamic parameters of state have different effect on the strength of hydrogen bonding. The correlations between H-bonds characteristics might be considered for different state parameters as indicator of changes in structure of H-bonded clusters no matter which kind of phase lines these parameters were obtained from. One

of such correlations, namely that between H-bond parameters and the mole fraction of H-bonded molecules ( $X_{\text{HB}}$ ), can be directly obtained from both IR spectroscopic data and computer simulations.

To the best of our knowledge, Barlow et al. [1] were the first, who studied hydrogen bonding phenomena in liquid and supercritical alcohols, analyzing the following correlations derived from IR studies: coefficient of integrated absorbance versus  $X_{\text{HB}}$  and position of OH vibrational mode,  $\bar{\nu}_{\text{OH}}$  versus  $X_{\text{HB}}$ . In their paper the term “probability of hydrogen bonding” ( $P_{\text{B}}$ ) was used instead but  $X_{\text{HB}}$  is equivalent to  $P_{\text{B}}$ . It was shown for 2-propanol, 1-butanol and somewhat for ethanol that these correlations, regardless of the phase conditions applied (spectra for isobar, isotherm have been measured for these alcohols), are approximated well by two linear functions with the bend at  $X_{\text{HB}} = 0.65 \pm 0.05$ . The reason for that, as proposed by authors of [1], is the existence of only one type of H-bonded  $n$ -mers, probably dimers, as  $X_{\text{HB}}$  is less than 0.6. The linear relationship of  $\bar{\nu}_{\text{OH}}$  with  $X_{\text{HB}}$  evidenced clearly the cooperativity effect during H-bonds formation: increasing of H-bonded clusters size results in the strengthening of H-bonds. Thus, the threshold for existence of multi-size H-bonded clusters in simple alcohols has been observed experimentally. The only exception was methanol, simplest of alcohols, for which it was impossible to establish corresponding spectroscopic data in supercritical state [1].

In our recent work [2], we have performed Molecular dynamics (MD) simulations of sub- and supercritical methanol near the saturation curve and the critical point (phase line 1 in Fig. 1). Using the geometry-energy H-bond criterion, we calculated the correlation between the peak position in H-bond energy distribution and  $X_{\text{HB}}$  for 16 methanol phase states (Fig. 2).

This correlation was shown to be in good agreement with the abovementioned correlations reported by Barlow et al. [1], with the bend observed at  $X_{\text{HB}} \approx 0.77$ , which corresponds to the vicinity of the critical point. Thus, computer simulations complemented spectroscopic measurements concerning new observed feature of hydrogen bonding, which is likely to be a common one for all lower aliphatic alcohols.

S. Krishtal (✉)  
Department of Inorganic Chemistry,  
Ivanovo State University of Chemistry and Technology,  
Pr. F. Engel'sa, 153460 Ivanovo, Russia  
E-mail: skrishtal@mail.ru

M. Kiselev · A. Kolker  
Institute of Solution Chemistry of the RAS, Akademicheskaya st.1,  
153045 Ivanovo, Russia

A. Idrissi  
Laboratoire de Spectrochimie Infrarouge et Raman (UMR CNR  
A8516), Université des Sciences et Technologies de Lille,  
59655 Villeneuve d'Ascq Cedex, France

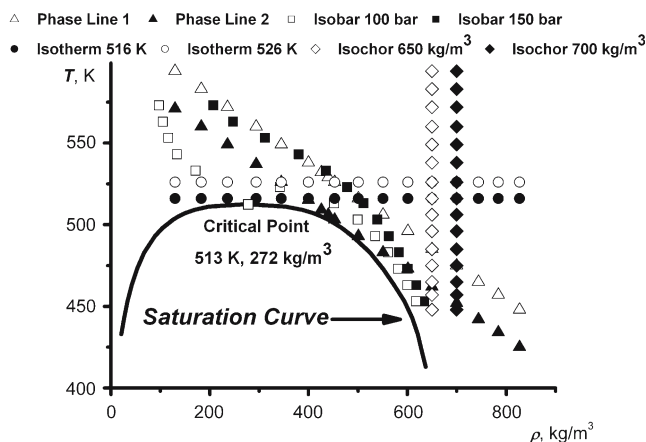


Fig. 1 Simulated methanol phase lines along with saturation curve [3]

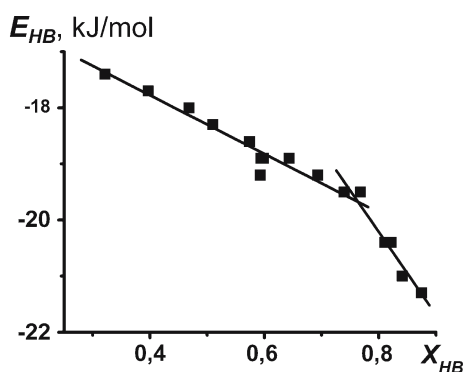


Fig. 2 Correlation between the peak position in H-bond energy distribution for the phase line 1 as shown in Fig. 1

Analysis of fractions of molecules with various H-bond numbers as functions of temperature as well as librational spectra at transition of methanol to supercritical state allowed to suppose that in methanol at  $X_{HB}$  less than 0.7 dimers dominate among H-bonded clusters and that in the vicinity of the salient point trimers are the main structure unit along with dimers.

A “classical” geometry-energy criterion of H-bond existence was used for H-bonding analysis. Here as the “classical” criteria we mean variety of H-bond definitions where interatomic distances, angles, interaction energies or H-bond lifetimes are employed for identification of H-bond existence. According to our criterion, two H1 methanol molecules [4] are considered H-bonded if the following conditions are satisfied:  $R_{OH} < 0.26$  nm and  $E_{HB} < -3KT$ . The quality of a given H-bond definition can be learned elsewhere [2,5]. While the studies of H-bonding phenomena were performed on the basis of a “classical” hybrid criterion, we have also tried to estimate the  $X_{HB}$  value, analyzing the charge transfer process occurred during H-bond formation. Studying H-bonding phenomena in supercritical state, one should realize that some controversies exist concerning the use of “classical” ad-hoc H-bond criteria in computer simulations of SCFs. First, the number of available experimental data on H-bonding in SCFs is not enough. Second, it is not clear whether the “classical” H-bond criteria usually established for ambi-

ent conditions are completely transferable on the case of SCFs because the dramatic structural and energy changes occur in supercritical state. At high temperature the interplay between kinetic and potential energy becomes crucial because kinetic energy of the molecules can exceed potential one and, as consequence, lifetimes of H-bonds become much shorter. On the other side, polarizability of molecules is essentially changed in SCFs and these changes are not imposed within “classical” H-bond criteria usually established for liquid-state H-bond systems. So, usefulness of quantum-chemical H-bond criteria for modeling SCFs is quite evident. At the same time, it appears that no studies of H-bonding in SCFs with quantum-chemical consideration of H-bond formation were reported up to date although quantum H-bond criteria exist for a long time.

In the present study, we have performed both extensive MD simulations of various phase lines near methanol saturation curve and the critical point and DFT calculations on classical MD configurations combined with the Natural bond orbital (NBO) analysis. The main goal of such detailed modeling sub- and supercritical methanol is to understand whether an H-bonded cluster structure mainly depends on thermodynamic parameters of state in some complex, non-trivial manner or it can be characterized by certain general factors (such as  $X_{HB}$ ) that have unambiguous relationship with the latter.

## 2 Combined quantum-chemical/classical MD study of H-bond formation in methanol

Popelier [6] introduced a number of quantum H-bond criteria based on the analysis of topological characteristics of the electron density distribution. He applied the above criteria for studying C–H...O [6] and dyhydrogen H-bonds [7]. Hobza et al. [8] used Popelier’s criteria to study H-bonding in various H-bond systems with an improper, “blue-shifted” H-bonds.

Another well-known approach to characterize quantum-mechanically the H-bonding process is the Reed–Weinhold NBO analysis [9], which allows detailing study of the intermolecular charge transfer process responsible for the H-bond formation. Weinhold et al. [9,10] performed numerous NBO-based studies of various H-bond systems, including water dimers, various H-bonded complexes, enzymes, etc. The advantage of the NBO analysis in studying H-bond systems also consists in opportunity to mark out the orbitals contributing to H-bond formation as well as to estimate the energy effects arising at interaction of these orbitals.

Thus, in compliance with all stated above, we have applied the NBO analysis to quantify the H-bond formation process in methanol under conditions far from ambient ones. The main point of interest was the phase state whose thermodynamic parameters correspond to the salient point on the correlation between  $E_{HB}$  and  $X_{HB}$  (Fig. 2). For this point on the phase diagram we have performed quantum-chemical studies of H-bonding, using introduced computational scheme, and

compared obtained results with those derived with “classical” H-bond criterion. We have then performed evaluation of the  $X_{\text{HB}}$  value in methanol by combining the DFT single point (SP) calculations on the classical MD configurations with the NBO analysis. As is known, the NBO analysis allows the studying of the charge transfer at H-bond formation. In our case and in accordance with the NBO concepts, the formation of H-bond is accompanied by charge transfer from oxygen lone-pair orbital of proton acceptor to non-Lewis valent anti-bond orbital of OH-bond of proton donor:  $\mathbf{n}_O \rightarrow \sigma_{\text{OH}}^*$ . In our studies we did not consider formation of H-bonds occurred through methyl hydrogens.

Stabilization energy is calculated from the second-order perturbation approach [10]:

$$E(2) = -\frac{n_O F_{\text{II}}^2}{\Delta E}, \quad (1)$$

where  $n_O$  is population of lone-pair orbital of proton acceptor,  $F_{\text{II}}$  – off-diagonal Fock matrix element,  $\Delta E$  – difference between energies of interacting NBOs.

Correspondingly, the charge transfer value at H-bond formation is calculated in the following way [10]:

$$q_{\text{CT}} = 2 \left( \frac{F_{\text{II}}}{\Delta E} \right)^2. \quad (2)$$

It is easy to show that  $E(2) \sim q_{\text{CT}}$  therefore, any of these properties may be used to characterize forming H-bond. For this purpose we used  $q_{\text{CT}}$ . It was shown by Weinfeld et al. that for an H-bond formation  $q_{\text{CT}}$  should exceed  $0.01 e$  [9, 10].

In our studies, we applied the NBO analysis to methanol instantaneous structures (I-structures) obtained from classical MD simulations on the basis of the following scheme:

1. Computer simulation with a classical potential model is performed and instantaneous molecular configurations are saved.
2. From these configurations, “clusters” consisted of a central molecule and some number of surrounding ones located inside of sphere with radius  $R$ , respectively central molecule, are selected in a random way.
3. Quantum chemical SP computations are performed on the selected clusters to calculate interactions from the first principles and the NBO analysis of the obtained wave functions is performed.
4. NBO analysis output is used to quantify the degree of H-bonding, i.e.  $X_{\text{HB}}$ .

Thus, the key approximation here is that the wave functions to be input for the NBO analysis are calculated on classical MD configurations. Wood et al. [11] and Sakane et al. [12] calculated free solvation energy of ambient water and free hydration energy of supercritical water, using a similar method called the ABC/FEP approach [11]. These authors showed experimentally measured energies to agree well with the calculated ones. It should be noted that, generally speaking, the results of the NBO analysis of selected clusters might depend on the number and size of clusters to be analyzed as well as on the potential model and ab initio method

used. Authors of [11] concluded that calculations of solvation energy of water with using of the abovementioned method both purely classical potential models and quantum-corrected ones, as the origins of instantaneous configurations, lead to similar results when several hundreds of configurations are taken into account.

As we assumed, the cluster size for a specific phase state depends on “saturation” of the electronic properties of the central molecule and three its nearest neighbors, i.e., those able to form H-bonds with the central one. In other words, the  $R$  value was chosen in such a way that its further increasing did not result in remarkable changes in natural charges at oxygen atoms and populations of NBOs participating in H-bond formation. For calculations of  $X_{\text{HB}}$  value, only the NBO analysis output for the central molecule and three of its nearest neighbors in each cluster were considered.

It should be noted that the analysis of an H-bond characteristics should not be necessarily limited to the central molecule and its nearest neighbors. Generally speaking, the number of molecules in each cluster suitable for quantitative estimations of H-bond parameters depends on the cluster size or, in other words, on the total number of molecules belonging to the cluster. Our calculations show that several tens of molecules in every cluster might contribute to estimation of H-bond parameters when the total number of molecules in the cluster approaches the value of 100. In that case it is even possible to evaluate the topological characteristics of H-bonded clusters in bulk methanol subject to a reasonable amount of clusters being analyzed.

As an illustration of our method, we present in this paper the results of calculation  $X_{\text{HB}}$  for methanol at 485 K and  $650 \text{ kg/m}^3$ , which corresponds to the salient point on the correlation between  $E_{\text{HB}}$  and  $X_{\text{HB}}$ . For 500 clusters QM SP computations have been performed with DFT B3LYP approach in variety of basis sets and the NBO analysis of the obtained wave functions was made. As a representative example, the results for one of the analyzed clusters are presented.

In Fig. 3 the  $q_{\text{CT}} \mathbf{n}_O \rightarrow \sigma_{\text{OH}}^*$  value from an environment to the central molecule and three of its nearest neighbors, as a function of the cluster size, is shown. In this case, the central molecule and three of its nearest neighbors could act as proton donors during an H-bond formation. It can be seen that at  $R \approx 0.7 \text{ nm}$  the so called saturation occurs, i.e., the further increase in  $R$  does not lead to considerable changes in the  $q_{\text{CT}}$  values.

In Fig. 4 dependence of natural charge at oxygen atom  $q_O$  of the same molecules on the cluster size is shown. Since the H-bond formation is due to the charge transfer from oxygen lone pair of proton acceptor, the change in  $q_O$  can be an indication of the formed H-bond, keeping in mind that in this case the central molecule and three of its nearest neighbors could act as proton acceptors. Again,  $R \approx 0.7 \text{ nm}$  can be satisfactory value as, when  $R$  exceeds it,  $q_O$  keeps relatively constant. Thus, the value of  $0.7 \text{ nm}$  has been chosen for the considered phase state as the sphere radius  $R$  for all clusters. This value corresponds approximately to 15–20 molecules in the cluster.

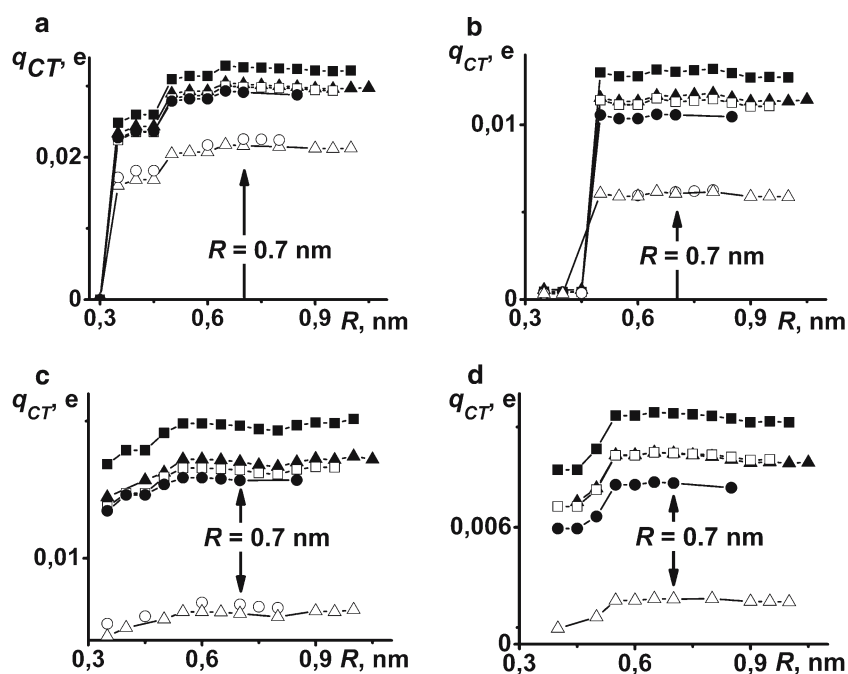


**Fig. 3** Charge transfer  $n_O \rightarrow \sigma_{OH}^*$  from environment to the central molecule **a**, its 1st **b**, 2nd **c**, and 3rd **d** nearest neighbors as a function of cluster size calculated in various basis sets: 6-31G\* (filled square), 6-31+G\*\* (filled triangle), 6-31++G\*\* (filled circle), cc-pVDZ (open square), cc-pVTZ (open triangle), cc-pVQZ (open circle)

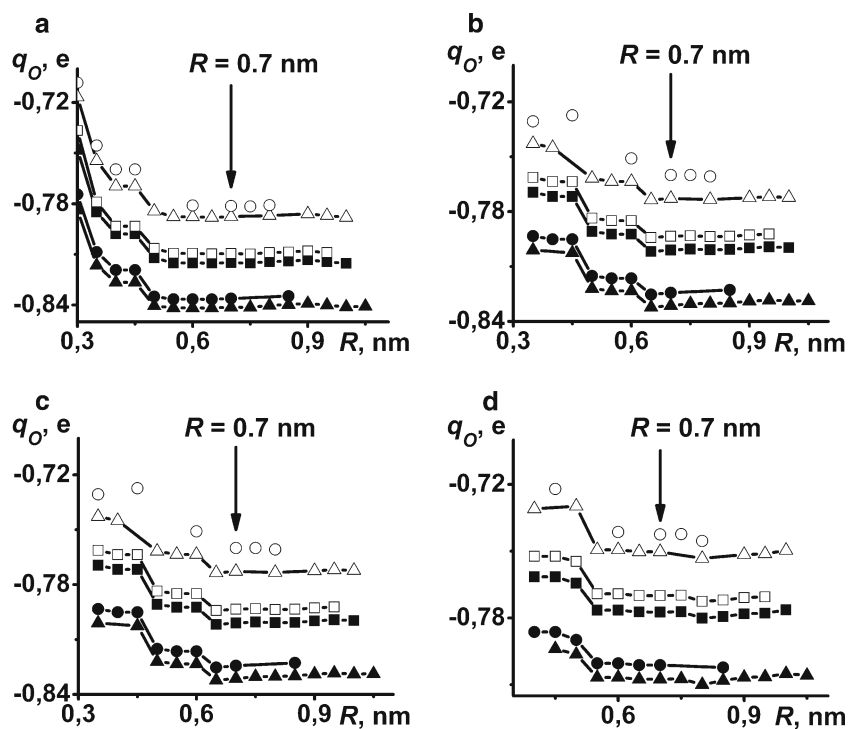


**Fig. 4** Natural charge at oxygen atom of the central molecule **a**, its 1st **b**, 2nd **c** and 3rd **d** nearest neighbors as a function of cluster size calculated in various basis sets: 6-31G\* (filled square), 6-31+G\*\* (filled triangle), 6-31++G\*\* (filled circle), cc-pVDZ (open square), cc-pVTZ (open triangle), cc-pVQZ (open circle)

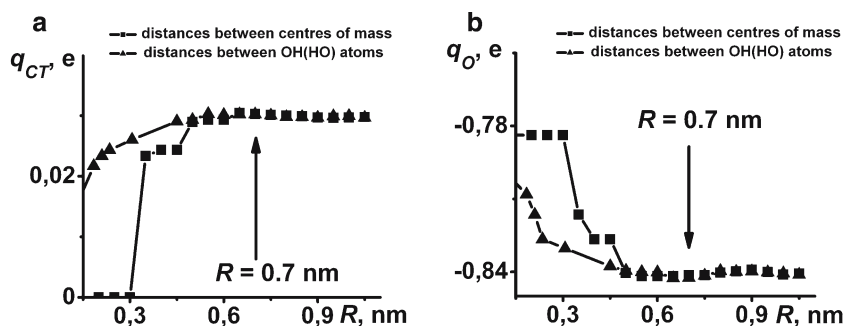


**Fig. 5** **a** The charge transfer and **b** natural charge at oxygen atom, calculated with different ways of selecting the surrounding molecules in clusters, as functions of cluster size

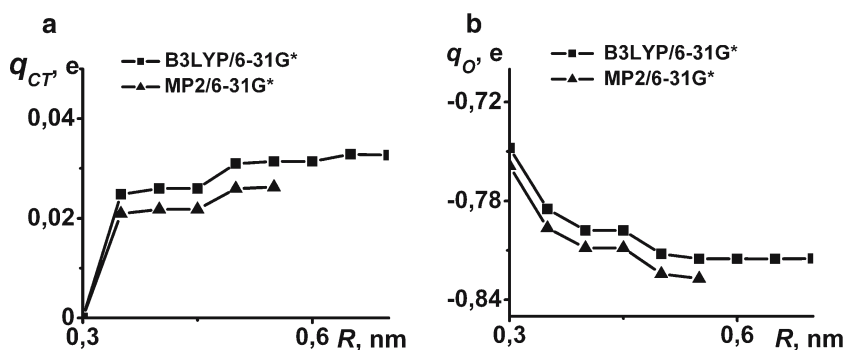


**Fig. 6** **a** Charge transfer value and **b** natural charge at oxygen atom, calculated with DFT B3LYP/6-31G\* and MP2/6-31G\* approaches, as functions of cluster size

We studied dependence of calculated  $q_{CT}$  and  $q_O$  values on the way of selecting the surrounding molecules in clusters. In Fig. 5 the results are shown for cases (1) when molecules are selected according to the center-of-mass distance between the central molecule and surrounding ones and (2) when molecules are selected according to the distance between OH (HO) atoms. As it is seen from the Fig. 6, differences do exist at  $R$  values less than 0.6–0.7 nm and disappear as  $R$  approaches value of 0.7 nm. Since  $R \approx 0.7$  nm has been chosen for a given phase conditions, the results will not depend on the way of selecting surrounding molecules. Further, the results calculated with using of center-of-mass separations between molecules in clusters are presented.

The comparison has also been made between the results of the NBO analysis obtained with different QM methods, namely, DFT B3LYP and MP2 approaches. In Fig. 6 the  $q_{CT}$  and  $q_O$  values depending on the QM method used are shown for one of the central molecules. This Figure shows that dependencies of  $q_{CT}$  and  $q_O$  values on the cluster size calculated from DFT B3LYP and MP2 methods are similar and shifted one relatively to other by the constant value. Alabugin et al. [13] used the NBO analysis for studying H-bond formation in  $\text{CF}_3\text{H} \cdots \text{OH}_2$  and  $\text{CF}_3\text{H} \cdots \text{Cl}^-$  dimers. As it was shown, "...The B3LYP results parallel the MP2 data quite closely..." [13]. We note that we did not perform comparison for larger basis sets. This figure is just for some additional knowledge about what happens if the MP2 level of theory is used in such calculations. As to BSSE, we think

that it has little effect on estimated  $X_{\text{HB}}$  values because we calculated the charge transfer value ( $q_{CT}$ ) rather than intermolecular interaction energy. We believe that BSSE influences  $q_{CT}$  not much because the latter is determined by a particle mean field.

In Fig. 7a the correlation between  $q_{CT}$  and intermolecular O–H distance for 50 randomly selected central molecules calculated in 6-31+G\*\* basis set is shown. It was assumed that the value of 0.01 e is the least one required for an H-bond formation [9,10]. In this connection, we adopted  $q_{CT} = 0.01$  e as the quantum criterion of H-bond existence. Figure 7a shows that  $q_{CT}$  values belonging to H-bonded molecules usually lie in between 0.01 and 0.03 e but in some cases can reach the values of 0.04 e and even 0.05 e and that some part of molecules seems to have no H-bonds on the assumption of the threshold charge transfer value being equal to 0.01 e. We can suppose that at least under phase conditions considered the O–H distance threshold value for H-bonds existence should be near 0.21 nm as it is predicted by charge transfer value estimations with the  $q_{CT}$  threshold being equal to 0.01 e and with B3LYP/6-31+G\*\* wave functions. For comparison, the  $R(\text{OH})$  threshold used in our "classical" criterion is equal to 0.26 nm under all phase conditions considered.

In Fig. 7b the correlation between  $q_{CT}$  and  $R(\text{OH})$  was shown only for those of central molecules selected from the above ones that are H-bonded according to our "classical" H-bond definition. Agreement between "quantum" and



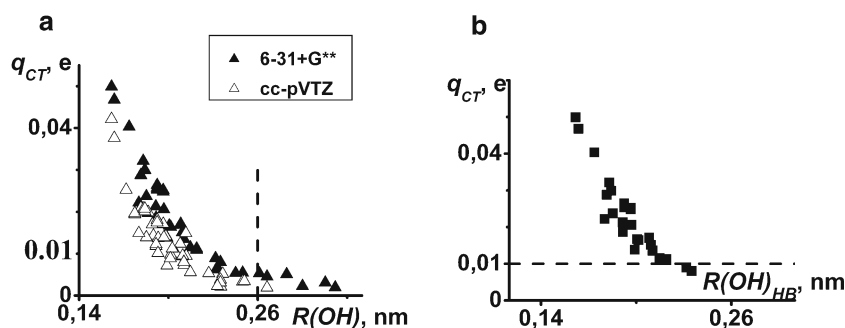


**Fig. 7** Correlations between **a** charge transfer value and intermolecular OH distance for 50 randomly selected central molecules and **b** charge transfer value for H-bonded, as stated by “classical” H-bond criterion, molecules and intermolecular OH distance. *Dashed lines* show  $R(OH)$  **a** and  $q_{CT}$  **b** threshold values used in our “classical” and “quantum” criteria, correspondingly

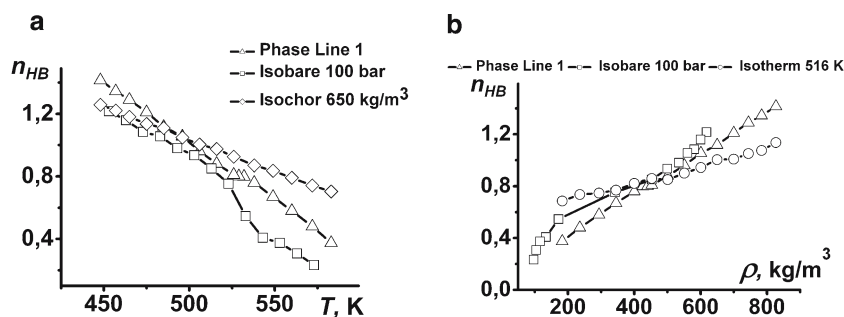


**Fig. 8** **a** Temperature dependence of mean H-bonds number for various methanol phase lines; **b** density dependence of mean H-bonds number for various methanol phase lines

“classical” definitions is quite well when 6-31+G\*\*  $q_{CT}$  values are used. Indeed, the correlation between the value of charge transfer and intermolecular distances is linear within “classical” criterion and it changes to be nonlinear when non-bonded molecules, from the point of view of both quantum and classical criteria, are considered (Fig. 8a). Moreover, the  $X_{HB}$  value calculated from the NBO analysis of B3LYP/6-31+G\*\* wave functions at 485 K and 650 kg/m<sup>3</sup> equals to 0.73, compared well with  $X_{HB} = 0.77$  as calculated within our “classical” H-bond criterion. The calculations with cc-pVTZ basis set result in smaller  $X_{HB}$  value of 0.69 and the latter is the least  $X_{HB}$  value obtained among basis sets under consideration.

Thus, we conclude that our hybrid “classical” H-bond criterion agrees well with the analysis of H-bonding based on charge transfer estimation within our combined ab initio/classical MD approach.

Analyzing results of our simulations of Phase line 1 (Fig. 1), we concluded that in the  $X_{HB}$  range of 0.70–0.77 ( $T=485$ – $506$  K) cooperative destruction of multi-size H-bonded clusters to monomers and H-bonded dimers takes place [2]. Then, the question of interest is whether similar structural transformations proceed regardless of the phase lines one considers or the different phase paths “dictate” their own conditions of changes in H-bonded clusters structure. To shed some light on this problem, we have analyzed temperature and density dependencies of a number of H-bond characteristics as well as their correlations with  $X_{HB}$  calculated along phase lines shown in Fig. 1. These characteristics

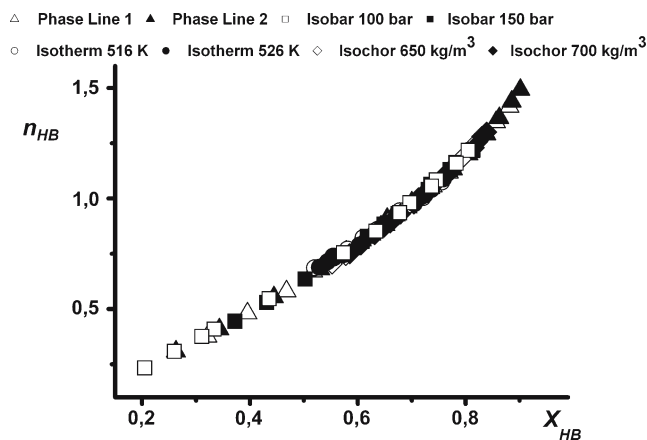


**Fig. 9** Correlations between average H-bonds number and mole fraction of H-bonded molecules ( $X_{HB}$ ) for various methanol phase lines

involve the mean H-bonds number  $n_{HB}$  and fractions of molecules with  $n$  ( $n=0$ – $2$ ) H-bonds,  $F_{1,2}$ .

There are number of studies where the authors demonstrated how density and temperature alter H-bonded clusters structure in supercritical methanol [14,15] and water [17]. While the generally accepted fact is that the number of H-bonds varies with temperature and/or density, the question whether the changes in hydrogen bonding in SCFs are primarily temperature or density dependent is still open. Asahi and Nakamura noted that “. . . the change in hydrogen bond number with density is larger than that with temperature in

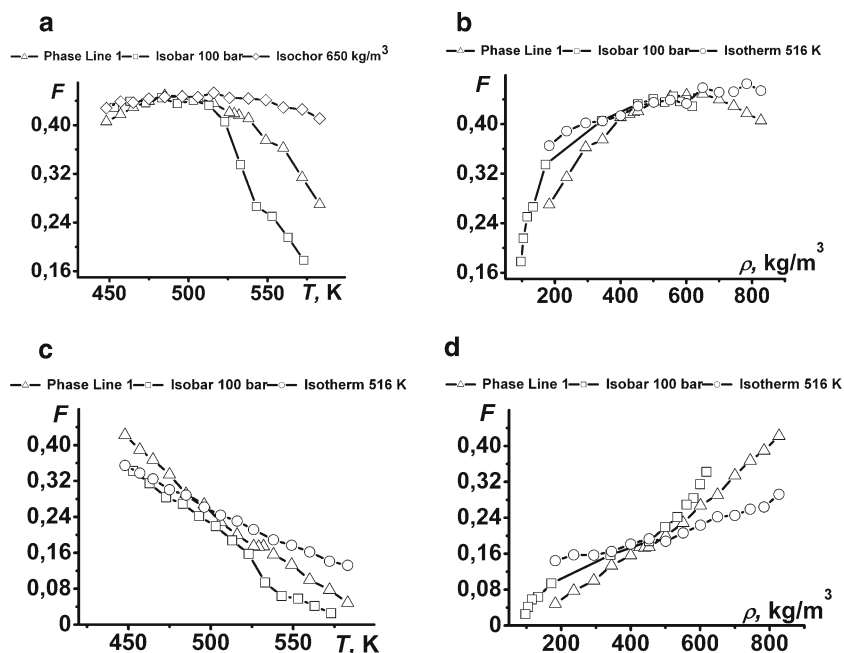


**Fig. 10** a and c Temperature dependencies of mole fraction of 1-bonded and 2-bonded molecules for various methanol phase lines; b and d density dependencies of mole fractions of 1-bonded and 2-bonded molecules for various methanol phase lines

the range of our study” [15]. At the same time, authors of [18] explained nonlinearities in behavior of H-bond parameters in near-critical water as a consequence of competition between structure-breaking effect of increase in temperature and structure-making tendency at the density decrease. Our analysis shows that, as expected, temperature and density have different effect on H-bond parameters depending on the phase path applied.

Figure 8 demonstrates  $n_{HB}$  as function of the state parameters for selected phase lines. Whereas the common tendency remains the same for all phase lines considered, i.e. temperature increase and decrease in density lead to the destruction of H-bonds and, as a consequence, to decrease in the  $n_{HB}$  value, the different combinations of temperature and density influence  $n_{HB}$  in a quantitatively different way. It can be seen that temperature and density dependencies of  $n_{HB}$  for phase line 1, isochor at  $650 \text{ kg/m}^3$  as well as isotherm at  $516 \text{ K}$  are close to be linear and that the slope of  $n_{HB}$  as function of temperature is less pronounced for the isochor than for the phase line 1 where both temperature and density are changed. Similarly, the slope of  $n_{HB}$  as function of density is less pronounced for the isotherm than for the phase line 1. Temperature and density dependencies of  $n_{HB}$  for the isobar have an inflection point near the critical point, i.e., at the state parameters corresponding to an inflection point on the phase diagram (Fig. 1), the function  $n_{HB}(T)$  for the isobar having the largest gradient among phase line considered.

Another picture arises if the correlations between  $n_{HB}$  and  $X_{HB}$  are examined (Fig. 9). In this case, the results for all considered phase lines fall into one curve, allowing unambiguous functional representation of these correlations.

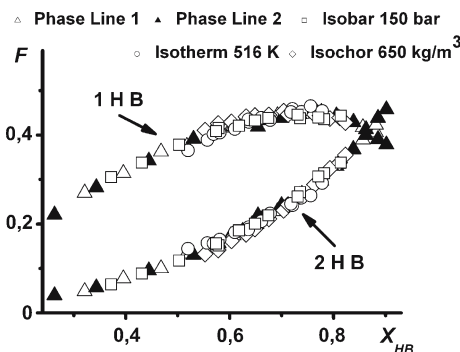


**Fig. 11** Correlations between mole fractions of molecules with one and two H-bonds and  $X_{HB}$  for various methanol phase lines

This is also the case if the fractions of one- and two-bonded molecules,  $F_{1,2}$  are considered (Fig. 10). Temperature dependencies of  $F_1$  for the phase line 1, isochor at  $650 \text{ kg/m}^3$ , and isobar at  $100 \text{ bar}$  have an extremum in the vicinity of the critical temperature, varying in the slope at temperatures higher than the critical one. Density dependencies of  $F_1$  for the isobar and the phase line 1 has an extremum as well, while that for the isotherm seems to have nothing. Temperature and density dependencies of  $F_2$  are similar to those of  $n_{HB}$  and, in general, the trend in the effect of state parameters on  $n_{HB}$  is virtually the same as the trend in the effect of state parameters on  $F_{1,2}$ , for the phase paths under consideration.

Further, it is interesting that the correlations between  $F_{1,2}$  and  $X_{HB}$  for given phase lines coincide with each other, as it was shown previously for the correlation between  $n_{HB}$  and

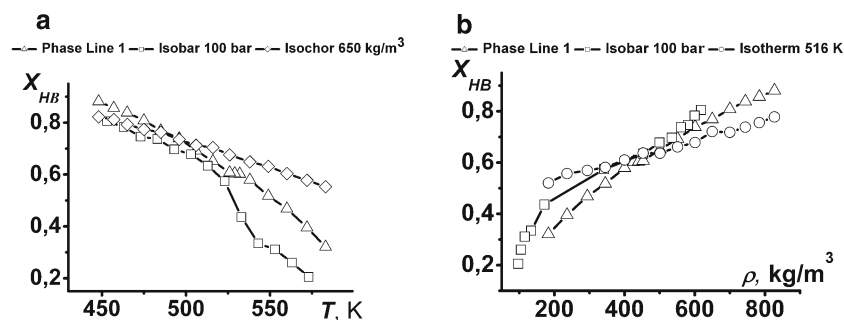


**Fig. 12** a Temperature and b density dependencies of mole fraction of H-bonded molecules  $X_{HB}$  for various methanol phase lines

$X_{HB}$  (Fig. 11). In other words, the functional type of these correlations does not depend on phase path methanol passes on at transition to supercritical state.

It should be noted that the  $X_{HB}$  value itself depends on the state parameters in a different way as it can be seen from Fig. 12 where temperature and density dependencies of  $X_{HB}$  calculated along studied phase lines are presented. Thus, the important conclusion concerning H-bonded clusters structure reorganization in near-critical methanol can be drawn as following: destruction of H-bonded clusters to monomers and dimers occurs at  $X_{HB}$  less than 0.7 regardless of the phase conditions applied, in a sense that it does not matter, in principle, how we change the state parameters to reach the  $X_{HB}$  threshold value, once it has been reached the multi-size clusters start to break up.

### 3 Conclusion

We report the results of our analysis of the effect of thermodynamic parameters of state on methanol H-bonded cluster (HBC) characteristics. Within the framework of these studies, extensive MD simulations of various phase lines near methanol saturation curve and critical point have been performed. Computer simulations demonstrated that despite expected different behavior of the HBC characteristics calculated along different phase lines, as functions of state parameters, the functional type of the correlations between topological HBC characteristics and the mole fraction of H-bonded molecules does not depend on the phase path methanol passes on at transition to supercritical state. In the present study, an attempt has been also made to estimate the mean H-bond number per methanol molecule by combining the DFT Single point calculations on classical MD configurations with Natural bond orbital analysis. Using our computational scheme, which is somewhat similar to the Wood's ABC/FEP approach [11], we tried to evaluate the degree of hydrogen bonding in bulk methanol at the phase point where

destruction of multi-size H-bonded clusters takes place, revealing itself as the bend in the correlation between the peak position in H-bond distribution and the mole fraction of H-bonded molecules.

**Acknowledgements** This work was supported by the Russian Foundation for Basic Research (grants no. 05-03-32850, 05-03-32696).

### References

1. Barlow SJ, Bondarenko GV, Gorbaty YE, Yamaguchi T, Poliakov M (2006) *J Phys Chem A* 106:10452–10460
2. Krishtal S, Kiselev M (2003) *Russ J Phys Chem* 77:1817–1820
3. Phase data for isobar lines and saturation curve were taken from: Zubarev V. N., Bagdonas A. V. *Teploenergetika (Moscow)* 1969, 16, 88.
4. Haughney M, Ferrario M, McDonald IR (1987) *J Phys Chem* 91:4934–4940
5. Krishtal S (2004) Structure of H-bonded clusters in methanol and water in Sub- and supercritical state. PhD Thesis, Institute of Solution Chemistry of Russian Academy of Sciences
6. Koch U, Popelier PLA (1995) *J Phys Chem* 99:9747
7. Popelier PLA (1998) *J Phys Chem A* 102:1873–1878
8. Hobza P, Havlas Z (2002) *Theor Chem Acc* 108:325–334
9. Reed AE, Curtiss LA, Weinhold F (1988) *Chem Rev* 88:899–926
10. Weinhold F (1997) *J Mol Struct* 398–399:181–197
11. Wood RH, Yezdimer EM, Sakane S, Barriocanal J (1999) *J Chem Phys* 110:1329–1337
12. Sakane S, Yezdimer EM, Liu W, Barriocanal JA, Doren DJ, Wood RH (2000) *J Chem Phys* 113:2583–2593
13. Alabugin IV, Manoharan M, Peabody S, Weinhold F (2003) *J Am Chem Soc* 125:5973–5987
14. Asahi N, Nakamura Y (1998) *Chem Phys Lett* 290:63–67
15. Yamaguchi T, Benmore CJ, Soper AK (2000) *J Chem Phys* 112:8976–8987
16. Kalinichev AG (2001) In: Cygan RT, Kubicki JD (eds) *Molecular modeling theory: applications in the geosciences. Reviews in mineralogy and geochemistry*, vol 42, Mineralogical Society of America, Washington, D.C, pp 83–130
17. Mountain RD (1999) *J Chem Phys* 110:2109–2115
18. Krishtal S, Kiselev M, Puhovski Y, Kerdcharoen T, Hannongbua S, Heinzinger K (2001) *Z Naturforsch* 56a:579–584